A R C H I V E S O F M E T A L L U R G Y A N D M A T E R I A L S
Volume 60 2015 Issue 3
DOI: 10.1515/amm-2015-0308

K. SIECZKOWSKI*, J. ADAMIEC*,#, G. SAWICKI**

THE STRUCTURE AND PROPERTIES OF MIXED WELDED JOINTS MADE OF X10NiCrAlTi32-21 AND X6CrNiMoTi17-12-2 STEELS

STRUKTURA I WŁAŚCIWOŚCI ZŁĄCZY MIESZANYCH SPAWANYCH ZE STALI X10NiCrAlTi32-21 ORAZ X6CrNiMoTi17-12-2

This paper describes the welding technology applied for mixed joints of tubes made of austenitic steels in the X10NiCrAlTi32 - 21 and X6CrNiMoTi17 -12-2 grades. One made a butt joint and a multi-run joint, with the inert gas welding method and a non-consumable electrode. The mechanical properties were tested in the following scope: static tensile test, bending test from the side of the face and from the side of the root, impact test of the joint and hardness measurements. The tests were supplemented by the assessment of the macrostructure and microstructure of the joint. The performed non-destructive and structural tests did not reveal any welding imperfections, and the mechanical test results confirmed high properties of the welded joint. On this basis, the joint was classified into the “B” quality level according to PN EN ISO 5817. The mechanical and structural test results constitute the basis for qualification of the welding technology according to PN EN ISO 15614 .

Keywords: mixed joint, TIG welding, austenitic steels

W pracy opisano technologię spawania złączy mieszanych rur ze stali austenicznych w gatunku X10NiCrAlTi32-21 oraz X6CrNiMoTi17-12-2. Wykonano połączenia doczołowe, wielościegowe, metodą spawania elektrodą nietopliwą w osłonie gazu obojętnego. Zakres badań właściwości mechanicznych obejmował: statyczną próbę rozciągania, próbę gięcia od strony lica i od strony grani oraz badania udarności złącza i pomiary twardości. Badania uzupełniono o ocenę makrostruktury i mikrostruktury połączenia. Przeprowadzone badania nieniszczące i badanie strukturalne nie ujawniły niezgodności spawalniczych, a uzyskane wyniki badań mechanicznych potwierdzają wysokie właściwości złącza spawanego. Na tej podstawie złącze zakwalifikowano do klasy jakości "B" według PN EN ISO 5817. Wyniki badań mechanicznych oraz badań strukturalnych stanowią podstawę do kwalifikowania technologii spawania wg PN-EN ISO 5817.

1. Introduction

A plan for development of the power industry in Poland till 2020 predicts in its “prosperity” version a substantial increase in energy consumption and in the related capital expenditures. Energy will be obtained mainly from the combustion of conventional fuels, renewable fuels and from the recovery of thermal energy. Most of the capital expenditures (60-70%) will be spent on modernizations and reconstructions of the existing power units and on the construction of new ones with supercritical and ultra-supercritical parameters [1]. This will require an application of high-temperature creep resistance and heat resistance materials, such as austenitic steels [2]. Joints made of high-temperature creep resistance austenitic steels should be characterized by good resistance to low cycle fatigue,

TABLE 1
Percentage share of the alloying elements in the material of the welded tubes

Material	% mass of the alloying elements						
	C	Cr	Mn	Ni	Al	Ti	S
X10NiCrAlTi32-21	0.064	20.65	0.63	31.1	0.47	0.53	0.001
X6CrNiMoTi17-12-2	0.050	16.52	1.60	11.82	-	0.39	0.003

* SILESIAN UNIVERSITY OF TECHNOLOGY, FACULTY OF MATERIALS ENGINEERING AND METALLURGY, 8 KRASINSKIEGO STR., 40-019 KATOWICE, POLAND
** ENERGOINSTAL S.A, 188 D. ROZDZIENSKIEGO AV., 40-203 KATOWICE, POLAND
# Corresponding author: janusz.adamiec@polsl.pl

due to their relatively high thermal expansion compared to ferritic steels, lack of welding imperfections, such as cracks or adhesions, and good mechanical properties [3]. The connecting technology should be qualified in accordance with the requirements of the PN EN ISO 15614 standard [4].

2. Test material

A tube of ϕ 48.3 in diameter and 5 mm-thick wall, made of X10NiCrAlTi32-21, as well as a tube ϕ 48.3 x 5, made of X6CrNiMoTi17-12-2, were the welding samples. The chemical composition according to the mill certificate is shown in Table 1. A welding wire of 2 mm in diameter, made of S Ni6082 (NiCr20Mn3Nb) steel grade was used as an additional welding material.

The welding tubes were bevelled at an angle of 60˚ (fig. 1a). The V- butt joint with a 2 mm threshold was performed with the TIG (141) method, using a direct current and linear energy of the arc not exceeding 1.2 kJ/cm, in argon shield, with the flow rate of 8-10 l/min. Figure 1.b presents the sequence of the beads. The interpass temperature did not exceed 150°C.

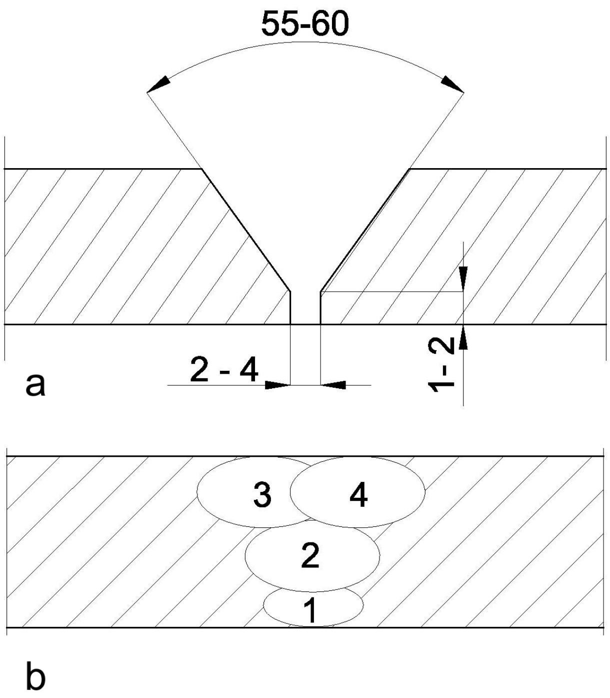

Fig. 1. Diagram showing a preparation of the joint for welding (a), sequence of the bead arrangement (b)

3. Test results and their analysis

3.1 Non-destructive tests of the joint

The visual tests were performed according to the requirements of the EN-ISO 17637 standard. The view of the face of the fusion weld is presented in Fig. 2. It was found that the joint had a correct even face. No black heat tints were revealed, which indicates a correct linear energy of the arc during the welding process.

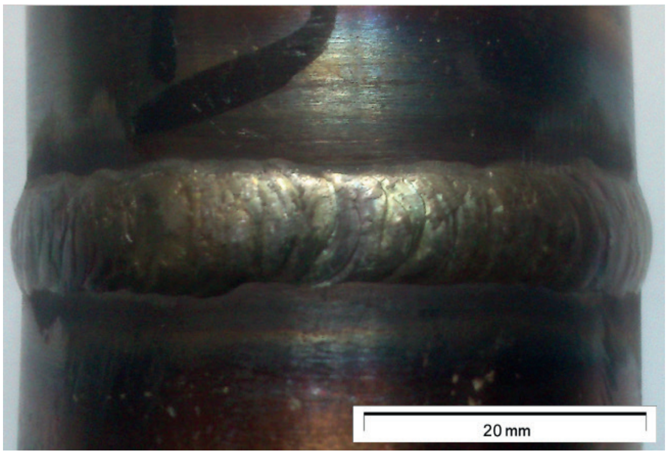

Fig. 2. Face of a mixed joint made of X10NiCrAlTi32-21 and X6CrNiMoTi17-12-2 steels

In order to reveal surface imperfections in the area of the joint, one performed liquid-penetrant inspections in accordance with EN 571-1. One used the Diffu-Therm BDR, Ch-No. 2112 dye penetrant, BRE-S, Ch. No. 7010 removal and BEA, Cr. No. 2313 developer. The exposure time at 20°C was 30 min. The observations were conducted with illumination of 550-650 Lx. The tests showed no discontinuities on the surface of the joint.

The liquid-penetrant inspections were supplemented by radiographic examinations performed in accordance with the requirements of the EN 1435 B standard. Kodak Eresco 42 MF3 X-ray lamp and Kodak T200 C4 film were used.

3.2 Joint hardness tests

Hardness of the joint from the side of the face and from the side of the root was measured according to the PN EN ISO 6507-1:2007 and PN EN 1043-1:2000 standards. The measurements were taken with the application of the HPO 250 hardness tester, with the Vickers method, at the load of 98 N (HV10). The results (the average of three measurements) are shown in Figure 3. The hardness distribution analysis showed that the hardness of the native material made of the X10NiCrAlTi32-21 steel ranged from 146 HV to 164 HV. A similar range of hardness was measured in the HAZ (heat affected zone), i.e. from 145 HV to 160 HV. The average hardness in the fusion weld amounted to 159 HV from the side of the face (from 154HV to 163HV) and 153HV (from 152 HV to 158HV) from the side of the root. Hardness in the heat affected zone in the tube made of X6CrNiMoTi17-12-2 steel ranged from 132 HV to 149 HV, and in the material it was 137 HV (from 130 HV to 142 HV) on average (Fig. 3). The hardness of the joint is correct, one revealed no cures of the joint areas of a difference exceeding 100 HV, which is a prerequisite for the application of the developed welding technology in the power industry (according to PN EN ISO 12592).

TABLE 2

Impact test results for a joint of the tubes made of X10NiCrAlTi32-21 and X6CrNiMoTi17-12-2 steels

No.	Place of sampling	Sample size, mm	Measurement of the rupture work J	Impact resistance J/cm^2
1	HAZ X10NiCrAlTi32-21	4x8	52	187
2			64	
3			63	
4	Fusion weld	4x8	59	187
5			62	
6			59	
7	HAZ X6CrNiMoTi17-12-2	4x8	64	187
8			56	
9			61	

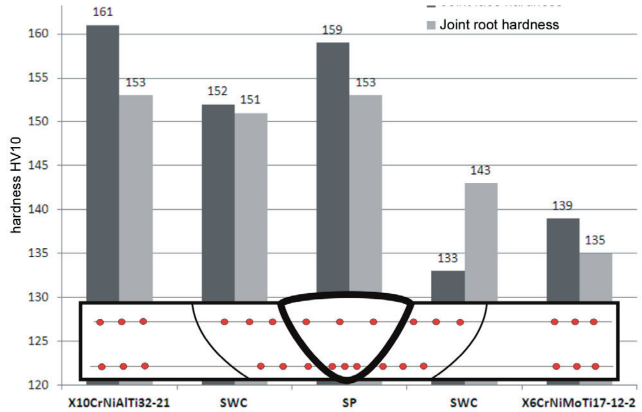

Fig. 3. Distribution of hardness in the joint on the line from the side of the face and from the side of the root

3.3 Assessment of the impact resistance of the joints

The impact test was performed in accordance with the requirements of the PN-EN 875:1999 standard. The tests were performed on smaller samples, as the base material measured 4x8 mm with the V notch. The fracture tests were performed with the Charpy PA30 impact hammer, with the initial energy of 300J and temperature of 21°C. The impact resistance results for the HAZ and for the fusion weld are shown in Table 2

Analysis of the fracture test results from 52J to 64J shows that in all zones the impact resistance amounts to 187 J/cm^{2,} which proves a high homogeneity of the plastic properties of the joint (Table 2).

3.4 Assessment of the strength properties of the joint

The strength of the joint was assessed on the basis of the results of the static tensile test and the bending test from the side of the face and from the side of the root. The tests were performed with the EU40 strength testing machine, with the maximum tensile force of 400 kN. The static tensile test was performed in accordance with the PN-EN 895:1997 standard, in the temperature of 20°C, on samples measuring 6.1 x 5 mm. The results are shown in Table 3. The bending tests from the side of the face and from the side of the root on a mandrel of 20 mm in diameter by an angle of 180° were performed on samples cut parallel to the axis of the joint in the temperature of 20°C, in accordance with the requirements of the PN-EN 910:1999 standard. The results are shown in Table 3.

TABLE 3

Static tensile test and bending test results for the joint

Static tensile test results				
Type of sample	Size, mm	Rupture strength, kN	Strength, MPa	Result
1	6.1x5	15.1	494.5	Rupture outside the fusion weld
2	6.1x5	14.6	479.5	Rupture outside the fusion weld
Bending test results				
Type of sample	Measures b0 x h0, mm	Bending mandrel, mm	Bending angle, o	Result
Face	17 x 5	20	180	positive
Face	16.5 x 5	20	180	positive
Root	16 x 5	20	180	positive
Root	16 x 5	20	180	positive

The strength test results show that the strength of the fusion weld is greater than that of the native material. The bending test results also show that the plastic properties of the joint are comparable to those of the native material.

3.5 Tests of the structure of the joint

The structural tests were performed on a surface perpendicular to the welding direction. After the sample had been cut out, it was ground and polished with abrasive papers and diamond pastes until one obtained a metallographic specimen. In order to reveal the structure, the samples were etched electrolytically in the HNO_3 water solution, with a voltage of 2V. The microstructure was examined with the application of an Olympus SZX-9 stereoscopic microscope at magnifications of up to 50 times, in the dark field technique. The revealed macrostructure is shown in Figure 4. Figure 5 shows the microstructure of particular zones of the joint, assessed in the bright field technique with the use of an Olympus GX71 microscope. The structural tests were complemented by observations with a scanning electron microscope in the secondary electron technique, which allows one to assess the topography of the structure (Fig. 6).

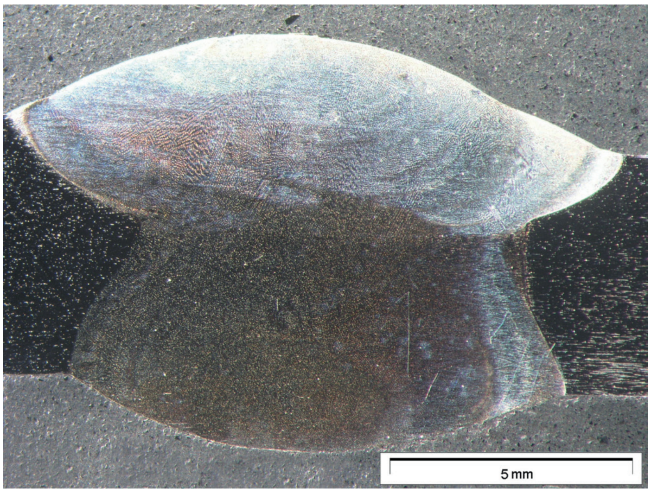

Fig. 4. Macrostructure of the mixed joint of the tubes made of X10NiCrAlTi32-21 and X6CrNiMoTi17-12-2 steels

The revealed macrostructure of the welded joint is correct and consists of three areas typical of welded joints, i.e. the native material (Fig. 4, C), a narrow heat-affected zone (Fig. 4, B) and the fusion weld area (Fig. 4, A). The shape of the fusion weld is normal, which is proved by the shape ratio (height to the width of the fusion weld) amounting to 1.2.

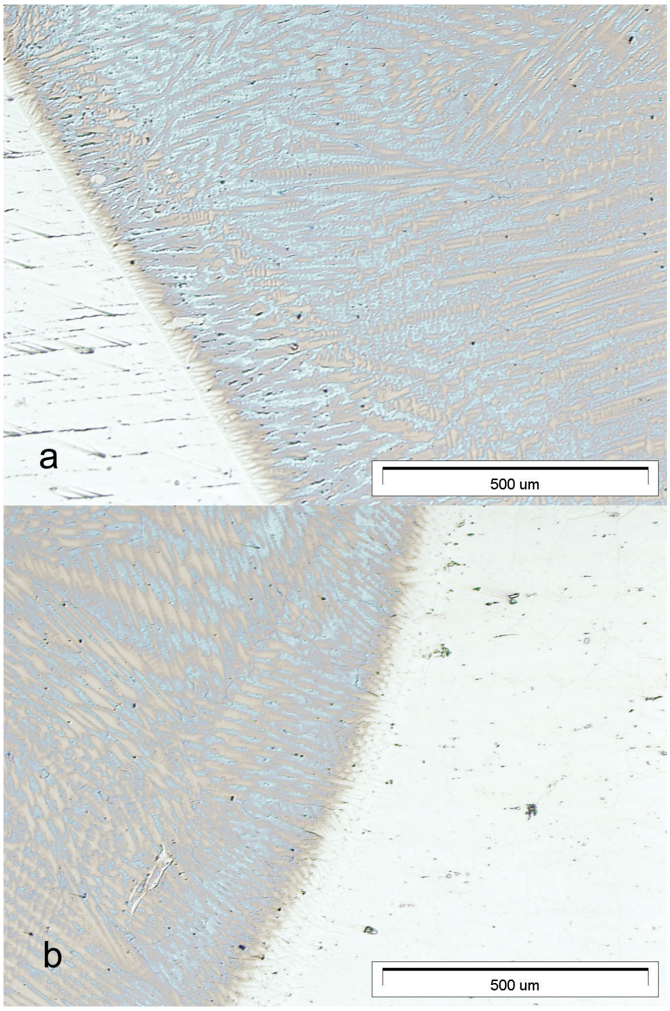

Fig. 5. Microstructure of the welded joint of the tubes made of X10NiCrAlTi32-21 and X6CrNiMoTi17-12-2 steels: a) fusion line from the side of the tube made of the X6CrNiMoTi17-12-2 steel, b) HAZ in the X10NiCrAlTi32-21 material

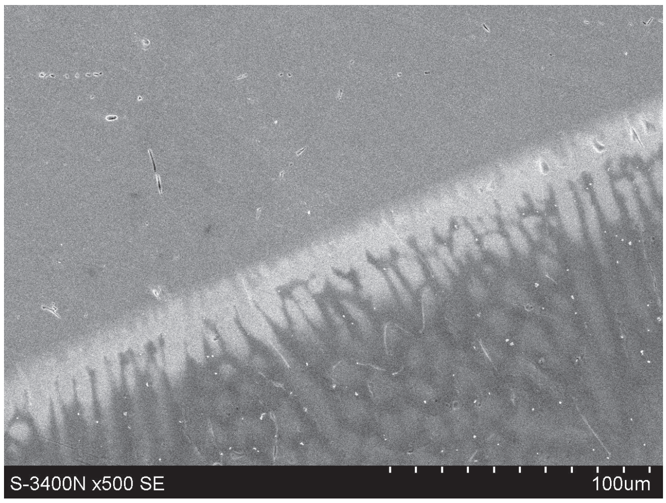

Fig. 6. Fusion line of the fusion weld into the tube made of the X10NiCrAlTi32-21 steel

The native material of the tube made of X10NiCrAlTi32-21 and of X6CrNiMoTi17-12-2 steel grades consists of elongated polygonal austenite grains in a band arrangement, typical of the rolling process (figure

5a, b). In the HAZ on the fusion line the grains of the native material become partially melted and fusion weld crystals build up epitaxially (fig. 5a, b). In this area one can also see partially melted boundaries of the austenite grains, which shows that the partial melting zone was about 10 µm wide (fig. 6). The fusion weld structure is mainly made up of column austenite grains, which build up in the direction of the heat abstraction.

Figure 7 shows liquation cracks. The occurrence of these cracks is conditioned on the presence of a liquid metal layer on the grain boundaries during the cooling process, when thermal tensile stresses develop [5].

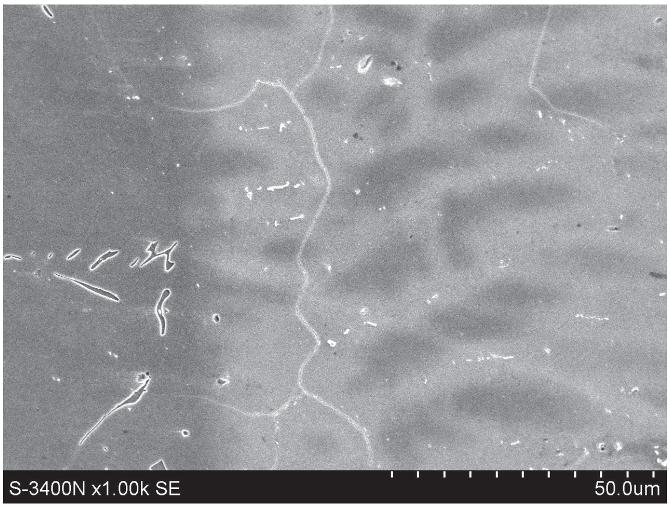

Fig 7. Liquation cracks in the HAZ of the fusion weld

With the application of the EDS unit, one made a linear distribution of the alloying elements in both fusion lines (Fig. 8). The share of nickel in the fusion weld is about 60%. The iron content in the fusion weld decreases, while the nickel content increases. One also revealed changes in the percentage amount of chromium in the HAZ from the side of the X6CrNiMoTi17-12-2 material. However the chromium content in the fusion weld is similar to that in the X10NiCrAlTi32-21 material.

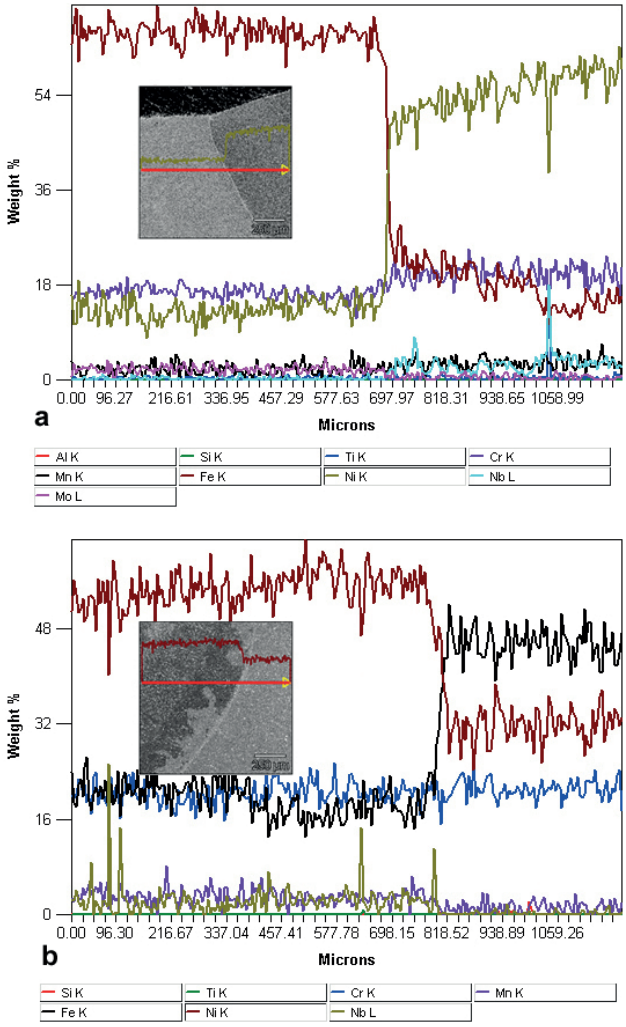

Fig 8. Linear distribution of the alloying elements: a) fusion line of the X6CrNiMoTi17-12-2 material, b) HAZ from the side of the X10NiCrAlTi32-21 material

Analysis of the linear distribution of the areal share of the elements showed a difference in the share of nickel and iron in the fusion weld between particular beads, where this content also changes inversely proportionally (Fig. 9).

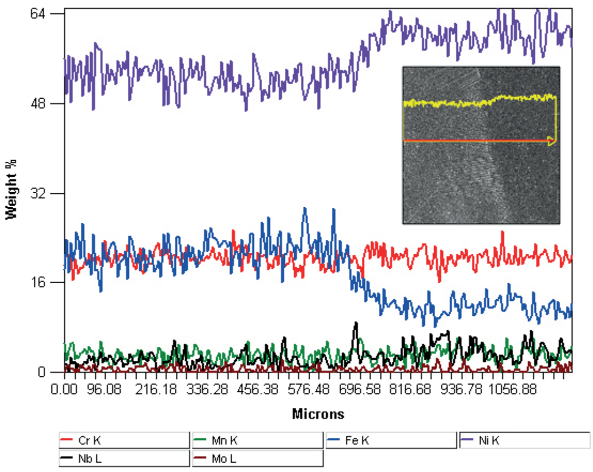

Fig. 9. Linear distribution of the elements on the fusion line between the layers of the applied fusion welds

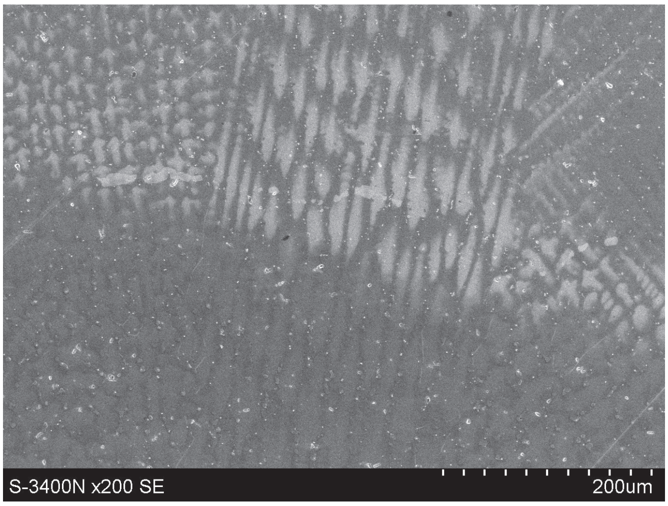

Fig. 10.Fusion line between the subsequent layers of the fusion weld

On the fusion line between the layers of the applied fusion weld, one can see the effects of the welding thermal cycle of the successively superimposed layers (Fig. 10). The occurring structures prove the existence of a dendritic and cellular crystallization. One can also see a changed crystallization direction in the form of elongated cellular- dendritic crystallites, formed following the change of the direction of bead arrangement [6].

The macro and microstructural examinations did not reveal and welding imperfections according to the PN EN 5817 standard, which allows one to classify the joint to the "B" level quality.

4. Conclusions

An increased demand for electricity in Poland results in the necessity to modernize old systems or construct new power units with supercritical parameters. Design of power units with supercritical parameters is associated with the application of materials characterised by a higher temperature creep resistance and heat resistance, such as austenitic steels.

The performed welding tests of tubes of ϕ 48.3 in diameter and wall thickness of 5mm, made of X10NiCrA1Ti32-21 and X6CrNiMoTi17-12-2 steels, showed that it was possible to get a correct joint with no welding imperfections. The joint has a smooth and even face (Fig. 3). No excess penetration bead or discontinuity from the side of the root were found. The fusion weld shape rate was at the level of 1.2 (Fig. 4). The structure of the joint consists of three typical areas, i.e. the native material made of polygonal austenite grains, a narrow heat-affected zone in which one can observe the process of partial melting of the grains and epitaxial crystalization of the crystals of the fusion weld, and of column crystals building up in the direction of the dissipation of heat in the fusion weld (Fig. 5).

The performed mechanical property tests showed that the rupture of the joint took place outside the fusion weld, and after bending on a 20 mm mandrel by an angle of 180°, one revealed no cracks from the side of the face and from the side of the root, which shows that the properties of the joint match those of the native material.

Analysis of the mechanical and structural test results allows one to qualify the technologies of welding of tube joints made of X10NiCrAlTi32-21 and X6CrNiMoTi17-12-2 steels in accordance with the requirements of the PN-EN ISO 15614-1 standard.

Acknowledgments

This paper was financed under the "Applied Research Programme" funded by the National Centre for Research and Development, project title: "The technology of laser welding of finned tubes made of austenitic steels and nickel alloys, intended for use in boilers with supercritical and ultra supercritical parameters", agreement no.: PBS1/A5/13/2012

REFERENCES

[1] E. Najgebauer, A. Patrycy, Zobowiązania polskiej energetyki wobec EU [Obligations of the Polish power industry towards the EU], www.geoland.pl

[2] J. Brózda, Stale energetyczne nowej generacji stosowane na urządzenia energetyki o parametrach nadkrytycznych i ich spawanie. Biuletyn Instytutu Spawalnictwa [Steels for power engineering applied inn the power industry equipment with supercritical parameters and their welding. Bulletin of the Institute of Welding], no. 5/2006

[3] J. Brózda, Stale żarowytrzymałe nowej generacji, ich spawalność i właściwości złączy spawanych, Biuletyn Instytutu Spawalnictwa [New generation high-temperature creep resistant steels, their weldability and properties of the welded joints, Bulletin of the Institute of Welding] no. 1/2004.

[4] PN-EN ISO 15614-1:2008/A1: Specyfikacja i kwalifikowanie technologii spawania metali – Badanie technologii spawania – Część 1- Spawanie łukowe i gazowe stali oraz spawanie łukowe niklu i stopów niklu [Specification and qualification of metal welding technologies - Welding technology testing - Part 1 - Arc and gas welding of steels and arc welding of nickel and nickel alloys

[5] P. Bernasovský, Contribution to HAZ liquation cracking of austenitic stainless steel, in: T. Böllinghaus, H. Herold, Hot cracking phenomena in welds, Springer, 2005

[6] E. Tasak, Metalurgia spawania [Metallurgy of welding], JAK Cracow 2009

Received: 20 October 2014.